# Development of Pulsed Laser Deposition
# System for the Formation of Web-liked Carbon Nanotubes

[1,2]Noorhana Yahya, [2]Beh Hoe Guan and [1,2]Mansor Hashim
[1]Advanced Materials Laboratory, Institute of Advanced Technology, University Putra Malaysia
43400 UPM Serdang, Selangor, Malaysia
[2]Department of Physics, Faculty of Science, University Putra Malaysia
43400 UPM Serdang, Selangor, Malaysia

**Abstract:** This work reports on our earnest effort to develop a pulsed laser ablation deposition system for the production of carbon nanotubes (CNTs). The correct condition such as the pressure, ablation time, power of laser will result in different structures and morphology of the tubes. A T-shaped stainless steel chamber was designed. Nd:YAG laser with 532 nm wavelength, 10.54W output power and pulsed width of 5-7 ns was used to ablate a pellet form graphite for 30 minutes. The morphology and the structural properties of the tubes were studied. The results were compared with graphite pellet filled with 10 weight % of Nickel as catalyst. It was found that an Argon environment with the Ni catalyst result in the formation of a web-like carbon nanotubes. XRD profile and TEM image confirmed the formation of CNTs.

**Key words:** Pulsed laser deposition system, web-liked carbon nanotubes

## INTRODUCTION

Carbon nanotubes emerged recently as unique nanostructures with remarkable electronic and mechanical properties. They have been intensively investigated for their fundamental and technical importance. The electronic properties of nanotubes are of great interest, but they also appear to be most challenging to be characterized because of the small dimensions of the tubes[1]. The mechanical (stiffness, strength, toughness), thermal and electrical properties of carbon nanotube materials enable a multitude of applications, from batteries and fuel cells to fibres and cables to pharmaceutics and biomedical materials. Scores of additional applications emerge when one thinks of blending nanotubes with other materials to improve existing properties or to provide new ones. Another broad area of application for nanotube-filled plastics are in EMI/RFI shielding, which has uses, in portable electronics and defense applications. If, as appears likely, good attenuation of electromagnetic radiation can be attained at nanotubes loadings in the order of 1% or less, good mechanical stability should be maintained, allowing it to be moulded[11]. This would represent a significant breakthrough in plastics and enable broadening of their uses. Other defense uses of nanotube composites are similarly significant such as radar-absorbing or modifying material for aircraft and missiles[2].

Ijima's discovery of the carbon nanotubes using high-resolution transmission electron microscope (HR-TEM) has initiated a flurry of studies in the growth of the CNTs. The effects of various processing conditions on the growth yield of CNTs was extensively studied by many researchers[3,5,7,8]. The formation of single-walled carbon nanotubes by laser ablation using CNiCo target, where the graphite pellet with some metal catalysts absorbs the laser beam, heat up and transforms into molten C, are studied. The yield of nanotubes formed by Nd: YAG laser ablation depends on the target composition with yields following the older $C_xNi_yCo_y > C_xNi_y \gg C_xCo_z$[4]. Historically, laser ablation was the first method used to produce fullerene nanostructures in the gas phase[3]. However, they were generally found to grow in the presence of metal catalysts. One of the main drawbacks of all methods is that the resulting material has an unsorted or rather randomly oriented structure. This hampers further investigations and applications of CNTs. This work reports our earnest effort to develop a pulsed laser deposition (PLD) system. Our hope is to obtain single walled CNTs using 10 weight % nickel metal catalyst. We compare our result with graphite pellet without any metal catalyst. Argon gas was used to ensure the inert environment. The presence of oxygen will result in oxidation process and as such, CNTs will not be produced.

## METHODOLOGY

We designed a PLD chamber with a port for the targets, pumping, substrates, gas inlet and quartz window for laser beam inlet. In Fig. 1, four dimensions are indicated: the laser port length, L; the target port

**Corresponding Author:** Noorhana Yahya, Advanced Materials Laboratory, Institute of Advanced Technology, University Putra Malaysia, 43400 UPM Serdang, Selangor, Malaysia

flange-to-target distance, T; the target to substrate distance, S; the substrate port flange-to-substrate distance, Z and the angle between the target normal (plume direction) and the laser beam, $\theta$[6].

The optimization of parameter S depends on the energy density, chamber pressure and target morphology. For most applications, S will be in the range 3 to 15 cm, although longer distances (~20cm) could be desirable to increase the surface area that is uniformed coated. By allowing S to be adjustable, optimized depositions can be obtained.

In this system, the material will find its way to all surfaces within the chamber, including the laser window, when a background gas is employed during the deposition. Material deposited on the window will interact with laser beam resulting permanent damage to the window. By increasing the length, L, of the laser port, the rate of material depositing on the window will be reduced. We designed the L length to be 15 cm.

The angle $\theta$ between the laser beam and the beam focal plane needs to be chosen such that the substrate holder and any other fixtures in the chamber will not be in the beam path. The angle should not be too small since the size and location of the spot is difficult to control near grazing angles. On the other hand, the angle cannot be too large since, eventually; the substrate holder will be an obstruction. An angle near $45^o$ was used in our designed target holder.

The manner in which the substrate is held and its location and orientation relative to the target are important parameters in a PLD system. The substrate must have good adhesion or epitaxy when the evaporants are collected on substrate. Bonding of the substrate to the substrate holder is important. We used silver paste to hold our substrate to the holder.

When the laser ablates the target materials, the evaporants are ejected as a highly forward-directed plume of material along the target normal plane. Subsequently, the substrate must be held directly opposite the target. The optimal target-to-substrate distance, S depends on several factors, the most significant of which is the energy delivered to the target. Higher beam energy permits larger S to be used. One might increase S rather than reduce the beam energy, with the deposition rate, the ability to adjust S is therefore designed.

A target was designed to easily access within the chamber so that mounting and demounting should be as simple as possible. To ensure uniformity of the deposition, a motor was connected to the target holder to rotate the target during ablation. A chamber window (Fig. 2) made of glass that has a diameter of about 15 cm, was designed to ensure the laser beam hits the target accurately. An Nd: YAG laser with a wavelength of 532nm and output power of 10.54W is used as energy (heat) source.
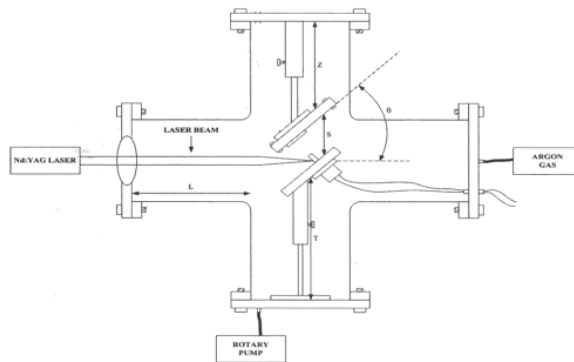


Fig. 1: A schematic experimental setup for the pulsed laser deposition (PLD) system
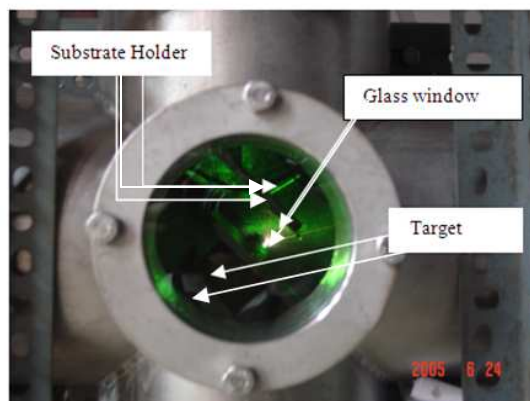


Fig. 2: A chamber window showing the Nd:YAG laser beam focusing onto a target material
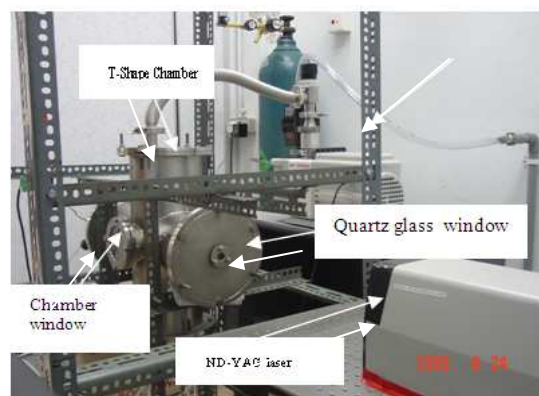


Fig. 3: Nd: YAG, PLD chamber and the rotary vacuum pump

A quartz glass window, as the laser beam inlet was used to ensure minimum absorption of the laser energy. A rotary pump is used to pump out the unwanted particle as well as the air inside the chamber to keep the vacuum condition. Existence of air would result in the oxidation process. Figure 3 exhibits our Nd:YAG laser, rotary vacuum pump and T-shaped chamber used in this experiment.
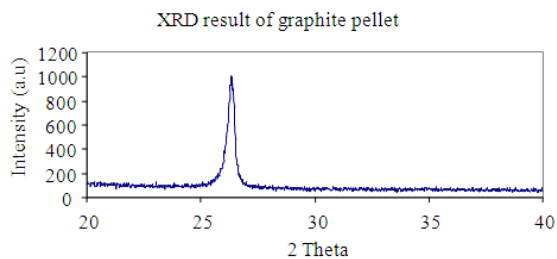
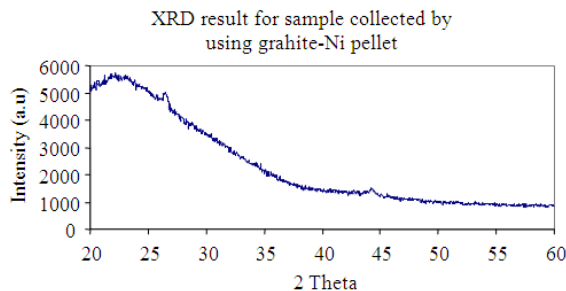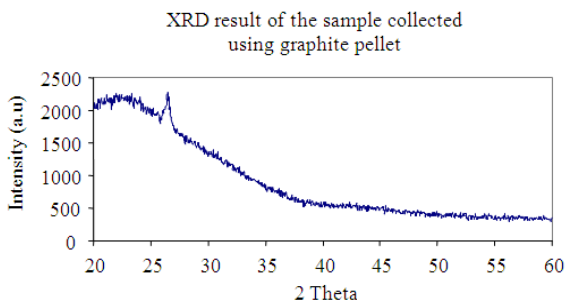Fig. 4:   XRD profile of the graphite pellet before laser ablation



Fig. 5:   XRD profile of the CNTs deposited on the glass substrate after laser ablation.
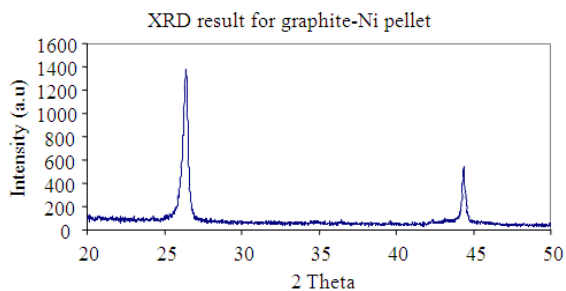


Fig. 6:   XRD profiles of the graphite pellet with 10 weight % of nickel catalyst before laser ablation
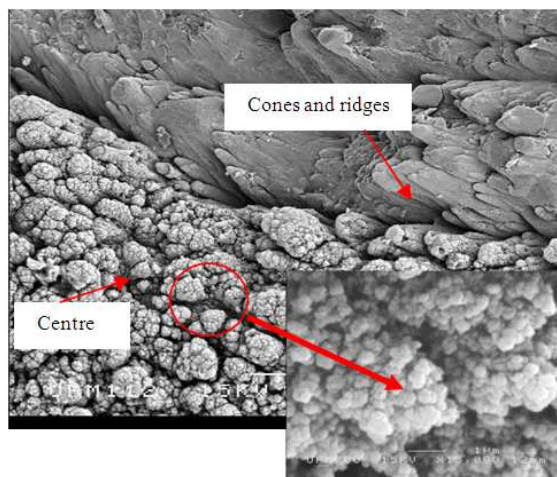
The pressure inside the chamber is about 80 mTorr after we vacuum out the air. We designed our substrate holder to hold the substrate and to collect the carbon particles ablated by the laser. We ablated the graphite pellet filled with 10 weight % of Ni as catalysts for 30 minutes. By changing some parameters such as, the pressure inside the chamber, the distance between substrate and target and the weight percent of catalyst, formation of carbon nanotubes can be achieved[7]. Scanning Electron Microscope (JEOL-MSZ-6400) with OXFORD INCA 300 Energy Dispersive X-ray Analysis (EDXA), Leo1455 Variable Pressure Scanning Electron Microscope (VPSEM) and X-Ray Diffractometry (Philips Expert Pro PW3040) were employed for examinations of the morphology and the phase of the target and the substrate.
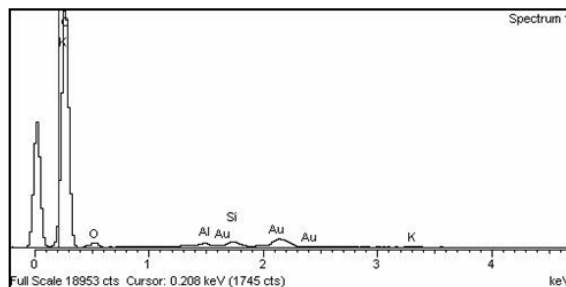


Fig. 7:   XRD profile of the CNTs with 10 weight % of nickel catalyst deposited on the glass substrate after laser ablation



Fig. 8:   SEM image of the Graphite target after laser ablation for 30 min



Fig. 9:   EDX profile for the graphite target after laser ablation in Argon gas

## X-RAY DIFFRACTION ANALYSIS

An XRD measurement ($2\theta$ scan) was carried out using $CuK_\alpha$ radiation to examine the structure of graphite as target (Fig. 4) and CNTs deposition (Fig. 5). Figure 4 shows the XRD profile of the graphite pellet before the ablation process was done. The spectrum of the graphite pellet reveals a sharp diffraction peak located at $26.39^o$ corresponding to the (002) graphite phase[7].
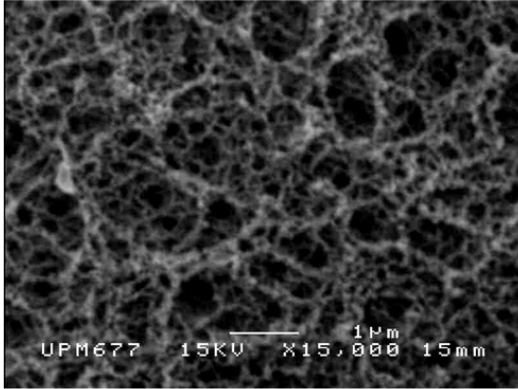
Fig. 10: SEM image of the deposition of CNTs after graphite pellet were ablated by the laser in an Argon gas environment
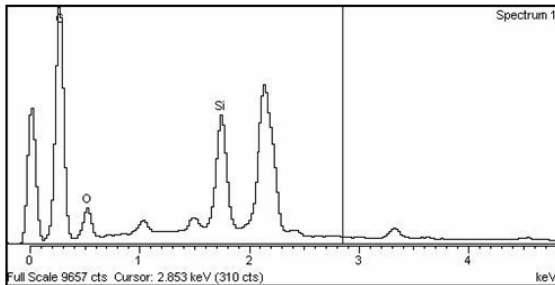


Fig. 11: EDX profile for the CNTs after laser ablation in Argon gas environment
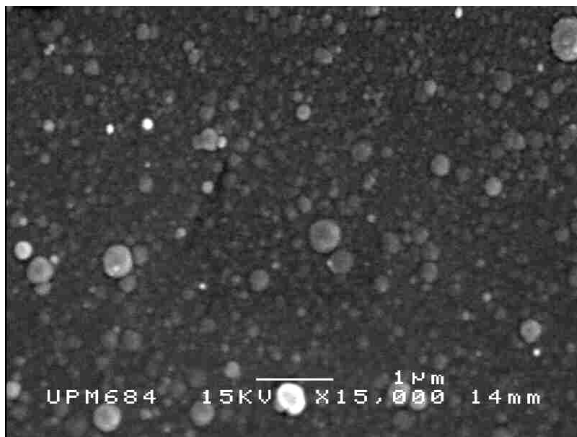


Fig. 12: SEM image of the deposition of sample collected after graphite pellet were ablated by the laser without Argon gas environment

The broadening of the peak in the XRD spectrum pattern was used by many researchers to estimate the particles size of the sample. The narrow peak will give a small distribution of particle size with large grain size[8]. The XRD spectrum of the graphite pellet showed narrow peak which indicates a small range of the particle size.
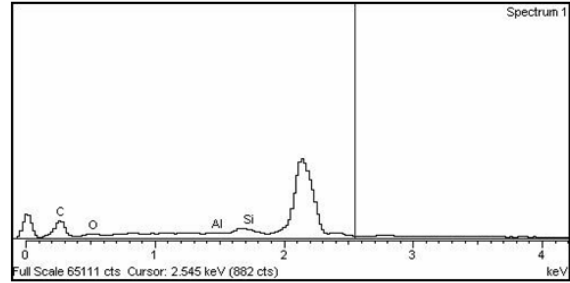


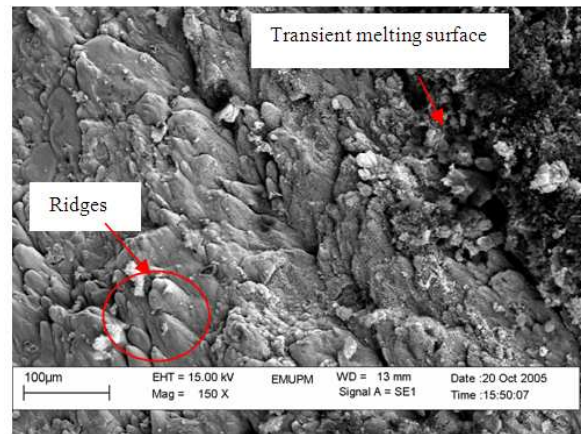Fig. 13: EDX profile for the deposited sample after ablation process without Argon gas



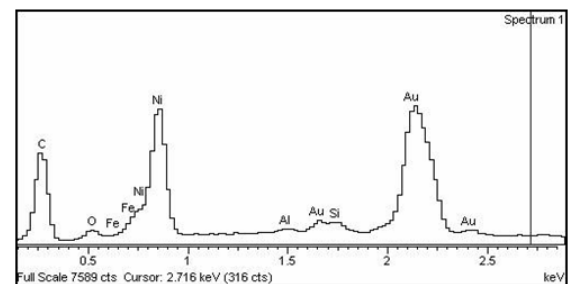Fig. 14: SEM image of the Graphite- Ni  target after laser ablation for 30 min



Fig. 15: EDX profile for the graphite-Ni target after laser ablation in Argon gas environment

Figure 5 shows the XRD profile of the deposited sample collected after the ablation process was done. The spectrum did not exhibit crystalline peaks. This peak is broad as a result of the nano-crystalline structure of the film[8]. We speculate randomly oriented carbon nanotubes were deposited on the surface of the glass substrate. In fact we speculate this is of the multiwall carbon nanotubes. The broad peak indicates different chirality in each of the nanotubes within the multiwall CNTs adding to our speculation of the broad peak.
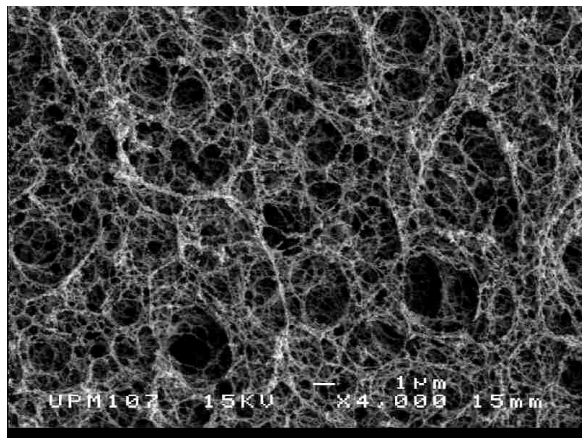
Fig. 16: SEM image of the deposition of CNTs with 10 weight % of nickel catalyst after graphite pellet were ablated by the laser in an Argon gas environment
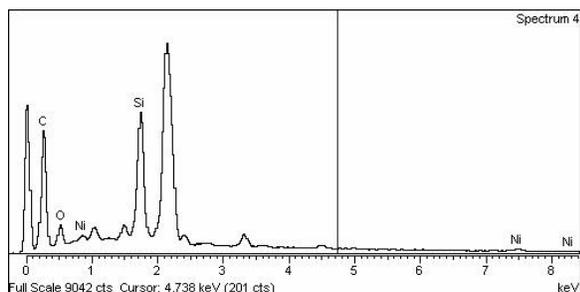


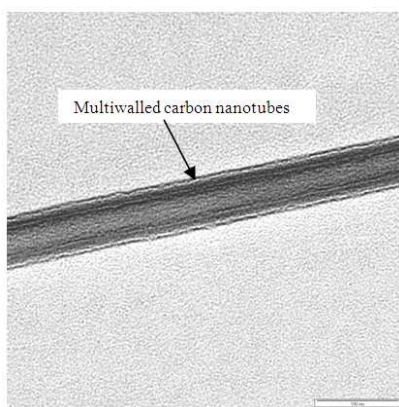Fig. 17: EDX profile for the CNTs deposition with 10 weight % of Ni catalyst in Argon gas



Fig. 18: TEM image of CNTs with 10 weight % of nickel catalyst after laser ablation process in Argon gas

The broad peak located at $22.60^o$, corresponds to CNTs phase[9]. Interesting however is the sharp peak located at $26.51^o$ which corresponds to (002) graphite phase was somewhat hidden by the broad CNTs peak.

Figure 6 shows the XRD profile for the graphite-nickel pellet. The spectra reveal two sharp diffraction

peaks. The first prominent peak, located at $26.42^o$ corresponds to the (002) graphite phase, where as the second peak located at $44.29^o$ corresponds to the Ni (111) phase.

Figure 7 shows the XRD profile of the deposited sample collected after the graphite- Ni target was ablated by the laser beam. The spectrum of the deposited sample also reveals two weak diffraction peaks. The first peak located at $26.48^o$ corresponds to (002) graphite phase[7] and the second peak located at $44.31^o$ corresponds to (011) Ni phase. The spectrum that demonstrates extremely broad diffraction peak, located at $22.38^o$, corresponds to CNTs phase[8]. The CNTs peak in the diffraction patterns deposited on the glass substrate is broad as a result of the nano-size particles. In addition, we speculate a random orientation of the CNTs was deposited on the glass substrate.

Having a closer look at Fig. 7 and 5 it is obvious that the deposited sample that was filled with Ni catalyst depicted higher counts/s for the CNTs peak. There has not been an effective way to determine the degree of alignment of the CNTs growth. However, XRD can be a useful tool to characterize the structural properties of the CNTs[9]. The detailed microscopic mechanism for the CNTs growth with catalytic effect is still lacking. We speculate that the deposition of the CNTs with Ni catalyst is more disordered comparable to the deposition of CNTs without any catalyst. The Ni particles as catalyst enhanced the rapid growth of the tubes during the ablation process. We speculate that the growth rate is so rapid that it did not have the time to self organize in such a way that the deposition is in disordered manner. The broader CNTs spectrum with higher intensity is a result of the catalytic growth[10].

Figure 8 shows the SEM image of the graphite pellet after laser ablation was done for about 30 minutes. SEM image shows the formation of cauliflower-liked carbon, cones and ridges on the side of the diameter of the rotated target ablated by 10.54W laser power with 4 torr argon gas pressure. Cauliflower-liked carbon was found to have formed in the center of the target. This is obvious as here is where the energy of the laser is maximum. When the target is exposed to longer and higher affluence of laser, a lot of energy will be transferred to the target. This energy will heat up the target to a very high temperature leading to the formation of the cauliflower-liked carbon on the target itself. This mechanism called exfoliational sputtering[6]. These transient melting surfaces will cause some of the materials at the target surface to be expelled from the target and deposited on the surface of the substrate. At the outer diameter of the center of the target where the lower Florence of the laser took place, cones and ridges are observed. Figure 9 depicts the EDX spectrum for the graphite target after laser irradiation. EDX result for the graphite target after laser ablation shows strong peaks of C, O, Al, K, Au and Si. The weight % of the sample for C, O, Al, K, Au and Si are 5.28, 87.06,0.49,

0.18, 6.23 and 0.77 respectively. The Al and K are speculated to be due to the impurities of the graphite starting powders and obviously Au is due to the gold coating.

Figure 10 shows the surface morphology of the deposited sample. It can be seen from this image that large quantities of carbon cluster deposited on the surface of substrate. The result show that a diameter size of the particles were formed ranging from 50nm-150nm. These observations are consistent with the result from the XRD study as shown by the broader diffraction peak.

Clear web-liked morphology was observed from the SEM image (Figure 10). We speculate the droplet of the molten expelled from the target surface collides with Argon gas and formed the carbon cluster and condenses on the surface of substrate. Without the present of the catalyst further growth of CNT is inhibited. EDX result (Fig. 11) of the deposited sample shows strong peaks of C, O and Si. The weight % of the sample for C, O, Si were 25.85, 71.68 and 2.47 respectively. Interesting however, is the absence of impurities such as Al and K, as we observed from the EDX of the target surface of the graphite pellet after ablation process.

The effect of the chamber environment was also scrutinized. We ablated our target without using Argon gas. Figure 12 shows the image with large quantities of spherical shaped particle scattered homogenously on the surface of the substrate. We attribute this to the slow rotation (~ 50 r.pm) of the target controlled by the motor which was connected to the target holder. The result show that a very broad size distribution, ranging from the few nm to 0.5 µm and diameter size of the carbon particles in this sample are larger than those forming the CNTs obtained using Argon gas. Without the presence of Argon gas, carbon species evaporate from the target and condenses on the substrate without undergoing collision with Argon gas.

Figure 13 shows the EDX spectrums for the sample collected from graphite pellet in the PLD process without using gas argon. EDX result of the tube in the cauliflower-liked carbon materials in shows strong peaks of C, Al, O and Si. The weight % of the sample for C, Al, O, Si are 26.79, 0.09, 72.34 and 0.77 respectively. The Al is results of impurities in the starting graphite powder and Au again, is due to the gold coating.

Figure 14 shows the SEM image of the graphite-Ni target after laser ablation. From the image, formation of cone and ridges are obvious. These transient melting surfaces will cause some of the materials at the target surface to be expelled from the target and deposited at the surface of the substrate. The reason for this mechanism was explained in the previous session. At the outer diameter of the center of the target where the lower Florence of the laser takes place, cones and ridges are observed.
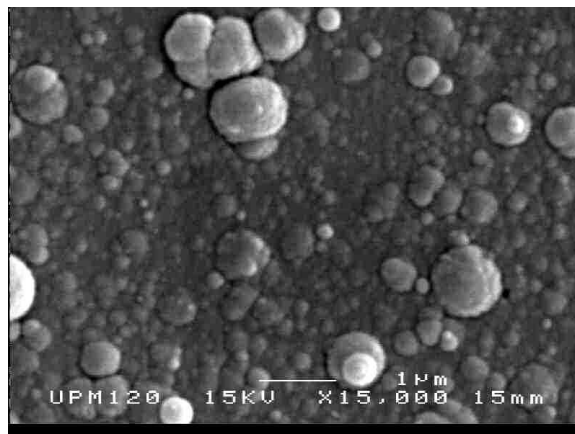


Fig. 19: SEM image of the deposited sample after graphite pellet with 10 weight % Ni were ablated by laser without Argon gas
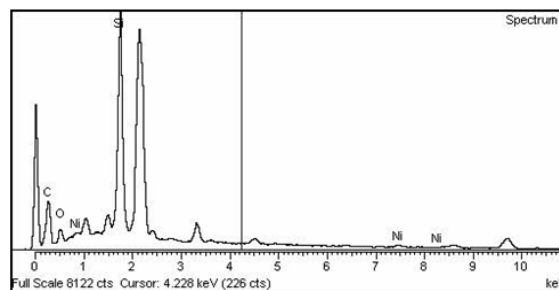


Fig. 20: EDX profile of the deposited sample after graphite pellet with 10 weight % Ni were ablated by laser without Argon gas

Figure 15 shows the EDX spectrum of graphite-Ni target after laser irradiated. From the EDX result high concentrate of the Ni on the surface of the cones, which comparable with the literature[11]. The melted surface are observed and the Ni scattered on the melted surface. Thin Ni layers were observed on the melted surface, which mean the carbon morphology is enough to reveal the Ni layer. When the target is exposed to longer or higher affluence of laser, a lot of energy will be transferred to the target. Graphite absorbs the laser beam heats up and transform into the molten C. Then the Ni particle in the target gains heat form and form a solution with the molten C. Droplets of the molten C containing the Ni catalyst are expelled from the target. The EDX results, clearly show that the Ni catalyst expelled from the target and play its role in the growth of the CNT.

Figure 16 shows the SEM image of the sample collected after the PLD process by using graphite-Ni pellet. It can be seen that large quantities of web-liked materials are deposited on the surface of substrate.

Very small size of the diameter of the tube on the web-liked material, ranging from 40nm-70nm. These

observations are consistent with the result from the XRD study as showed by the broader diffraction peak. Figure 17 shows the EDX spectrum of the sample collected from the PLD process by using graphite-Ni pellet. Strong peaks of C, Ni, O and Si with weight % of 24.53, 0.41, 70.57 and 4.48 respectively. The EDX profiles give us strong evidence that Ni catalyst were expelled from the target and effectively works as the catalyst to enhance the growth of the CNTs.

Transmission electron microscope (TEM) was employed to further confirm the formation of CNTs. Figure 18 reveals that the CNTs is a multiwall type with about 60-70 nm of diameter. The TEM image is consistence with the SEM image of the CNTs (Figure 16). We speculate the formation of the multi-walls are due to the high energy of the laser and the correct distance (S) of the target to substrate.

Figure 19 shows the SEM image of the sample after the ablation of laser without using gas argon. It can be seen from this image that large quantities of regular spherical particles were formed on the surface of substrate. The result shows a broad size distribution, ranging from the few nanometers to few µm. Figure 20 shows EDX spectrums of the spherical shaped morphology of carbon. The weight % of the sample for C, Ni, O, Si are 19.90, 0.55, 67.22 and 12.34 respectively. We could deduce that Ni plays its role as a catalyst to expel the graphite-Ni mixtures droplet from the target surface (Fig. 15), during the ablation process. On the other hand, the absence of Argon gas to provide the inert condition fails to produce the web-like CNTs. Interesting however is the diameter that was observed is larger than those without Nickel catalyst. The Ni somewhat acts as catalyst to enhance the growth of the spherical shaped-carbon. We speculate Ni metal received a large amount of energy and as a result, it melts and enhances the growth rate of the spherical carbon resulting in larger diameter of the spherical-liked carbon structures (Fig. 19).

## CONCLUSION

Carbon nanotubes were successfully synthesised via PLD system due to the suitable conditions, namely, the laser power (10.54W), ablation time (30 minutes), the argon gas environment, the pressure (4 Torrs), as well as the effect of 10 weight % nickel catalyst. The formation of CNTs was identified by the XRD profile and the SEM image. The TEM image supports our results. Of all the conditions, the formation of the CNTs is highly depended on the role of the Ni metal catalyst and the argon environment.

## REFERENCES

1. Yahya, N., M.H. Saad, I. Ismail, H.G. Beh, M.S.E. Shafie, R.B. Doshi and A.N. Zainal Abidin, 2004. Carbon Nanotubes: An Overview. Mag. of Phys., Sci. and Ideas, 4: 30.
2. Meyyappan, M., 2005. Carbon nanotubes. Science and Applications. Florida: CRC Press, Inc.
3. Huczko, A., 2002. Synthesis of aligned carbon nanotubes. Appl. Phys. A, Mater. Sci. and Process., 74: 617-638.
4. Yudasaka, M., T. Ichihashi and S. Iijima, 1998. Physical Chemistry, B, 103: 4345.
5. Thomas, W.E., 1997. Carbon Nanotubes: Preparation and Properties. Florida: CRC Press, Inc.
6. Chrisey, D.B and G.K. Hubler, 1994. Pulsed Laser Deposition of Thin Films. New York: John Wiley and Sons.
7. Ju, Y., F.Y. Li and R.Z. Wei, 2005. Catalytic growth of carbon nanotubes with large diameters. J. Serb. Chem. Soc., 70: 277-282.
8. Heiman, A., E. Larkin, E. Zolotoyabko and A. Hoffman, 2002. Microstructure and Stress in nanocrystalline diamond films deposited by DC glow discharge CVD. Diamond and Related Materials, 11: 601-607.
9. Cao A., A. Xu, L. Ji, D. Wu and B. Wei, 2001. X-ray diffraction characterization on the alignment degree of carbon nanotubes. Chem. Phys. Lett., 344: 13-17.
10. Park, J.B., G.S. Choi, Y.S. Cho, S.Y. Hong, D. Kim, S.Y Choi, J.H. Lee and K. I. Cho, 2002. Characterization of Fe-catalyzed carbon nanotubes grown by thermal chemical vapour deposition. J. Crystal Growth, 244: 211-217.
11. Haydari, M., M.M. Moksin, N. Yahya, W.M.M.Yunus and V.I. Grozescu, 2005. Thermal Wave Study on Carbon Nanotube-filled polymer Films at Low Temperatures by Using Flash Technique. Am. J. Appl. Sci., (Sp. Iss.)., pp: 49-52.